Geomicrobiology Journal, 20:15–24, 2003

0149-0451/03 $12.00 + .00
DOI: 10.1080/01490450390144349

Taylor & Francis
Taylor & Francis Group

Iron-Rich Diagenetic Minerals are Biomarkers of Microbial Activity in Antarctic Rocks

JACEK WIERZCHOS

Servei de Microscopia Electronica
Universitat de Lleida
c/Rovira Roure, Lleida, Spain

CARMEN ASCASO

Centro de Ciencias Medioambientales
CSIC
c/Serrano, Madrid, Spain

LEOPOLDO GARCÍA SANCHO

Fac. Farmacia
Universidad Complutense
Madrid, Spain

ALLAN GREEN

Biological Sciences
Waikato University
Hamilton, New Zealand

The cold, dry ecosystems of Antarctica have been shown to harbor traces left behind by microbial activity within certain types of rocks, but only two indirect biomarkers of cryptoendolithic activity in the Antarctic cold desert zone have been described to date. These are the geophysical and geochemical bioweathering patterns macroscopically observed in sandstone rock. Here we show that in this extreme environment, minerals are biologically transformed, and as a result, Fe-rich diagenetic minerals in the form of iron hydroxide nanocrystals and biogenic clays are deposited around chasmoendolithic hyphae and bacterial cells. Thus, when microbial life decays, these characteristic neocrystalized minerals act as distinct biomarkers of previous endolithic activity. The ability to recognize these traces may have potential astrobiological implications because the Antarctic Ross Desert is considered a terrestrial analogue of a possible ecosystem on early Mars.

Keywords Antarctic granite, biomarkers, cryptoendoliths, microfossils

Received 30 May 2001; accepted 10 October 2002.

Thanks are due to K. Nealson for critical reading of the manuscript, two anonymous reviewers for constructive comments, and A. Burton for the English revision. This study was funded by grant number ANT99-0680-C02-02 of the *Plan Nacional I + D* and *PGC* BOS2000-1121.

Address correspondence to Jacek Wierzchos, Universitat de Lleida, c/Rovira Roure, 44, 25198, Lleida, Spain. E-mail: jacekw@suic-me.udl.es

Introduction

One of the most outstanding features of life on the Antarctic continent is the predominance of rocks as substrates for living organisms (Friedmann 1982; Friedmann et al. 1988; Kappen 1993). Any discrete, unfavorable change in external conditions can result in the death of microscopic organisms, which may be followed by their disappearance possibly leading to trace microfossil formation. The sequence of events leading to the extinction of life in the Antarctic desert is considered to be a terrestrial analogue of the disappearance of possible life on early Mars (McKay et al. 1992). On these grounds, it is proposed that the investigation of such ecosystems could serve as a starting point for the development of methodologies, preparative techniques, and new technologies aimed at detecting and evaluating traces of life such as microfossils and biomarkers.

To date, only two biomarkers of the past activity of cryptoendoliths have been described: one is the geophysical bioweathering of rock surfaces forming characteristic exfoliation mosaic patterns (Kappen 1993; Sun and Friedmann 1999) and the other, the geochemical bioweathering patterns resulting from iron leaching observed in the surface layers of sandstone rocks (Friedmann and Weed 1987). However, both of these biomarkers have been observed macroscopically. It is clear that much further work is required in the detection of traces of past life in Antarctic rocks. Although the study of microorganisms colonizing the inside of lithic materials confronts with considerable difficulties, the detailed mineralogical and biological characterization of endolithic niches is essential for understanding the dynamic relationships between rock-dwelling microorganisms and their microhabitats. Recently, scanning electron microscopy with backscattered electron imaging (SEM-BSE) was successfully combined with microanalytical procedures (such as energy dispersive X-ray spectroscopy [EDS]) for the in situ study of endolithic microorganisms (Ascaso and Wierzchos 1994; Wierzchos and Ascaso 1994; Ascaso et al. 1995). Such an approach also permits the chemical characterization of mineral features (Wierzchos and Ascaso 1996). Here we report the use of SEM-BSE combined with EDS visualization and microanalytical strategies to provide substantial information on biologically transformed minerals in granitic rock from Antarctica. Using high resolution transmission electron microscopy (HRTEM) on previously SEM-BSE-EDS examined microzones separated from the polished blocks, we were able to observe relationships between microorganisms and minerals around chasmoendolithic communities on the spatial nanometer scale (Wierzchos and Ascaso 1998).

Materials

Pieces of granitic rock colonized by epilithic lichen thalli of *Lecidea cancriformis* (Dodge et Baker) were collected from the Ross Sea coast, Granite Harbour (77° 00′ S, 162° 34′ E). The taxonomy of this lichen is according to Øvstedal and Lewis Smith (2001). Mean air temperature ranges from −3.1°C (warmest month) to −26.1°C (coldest month) and relative humidity is 20 to 80% during the austral summer season (1999/2000). Mean annual precipitation, falling as snow, is 130 mm (rainfall equivalent). Mineralogical examination of this material demonstrated the presence of quartz, orthoclase, and plagioclase as the main minerals, and biotite, zircon, and apatite as accessory minerals. Small fragments of granitic rock with subsurface layers containing cryptoendolithic microorganisms were collected under natural conditions and stored at −20°C until processing for microscopy and microanalytical procedures.

Methods

SEM-BSE and EDS

Samples were processed for the in situ visualization of the rock-microorganisms interface by SEM operating in BSE emission mode. Details of this preparative procedure are given in Wierzchos and Ascaso (1994). Briefly, the SEM-BSE method involves two stages. The first is the sample preparation procedure, which includes glutaraldehyde fixation and osmium tetroxide and/or uranyl acetate staining techniques and the preparation of finely polished blocks containing resin-embedded rock samples. The BSE signal is strongly dependent on the mean atomic number of the target (Joy 1991). Thus, the SEM-BSE procedure not only enables samples with different inorganic features to be visualized, but also allows the identification of ultrastructural elements of the microorganisms by staining with heavy metals. The second stage involves visualization of the carbon coated biological-mineralogical transverse (perpendicular to the rock surface) sections using the BSE detector.

The energy dispersive X-ray spectroscopy (EDS) system coupled to the SEM-BSE instrument permitted the chemical characterization (qualitative and quantitative analysis of elements including spatial distribution images and line scans) of mineral features (Wierzchos and Ascaso 1996; Wierzchos and Ascaso 1998). Transverse sections of the finely polished blocks of rock were examined using a DSM 942A Zeiss instrument equipped with BSE solid state detector and an EDS microanalytical system (Link ISIS). Microscopy and analytical operating conditions were as reported by Wierzchos and Ascaso (1996).

HRTEM

In order to explore the bio-induced mineral transformation process by HRTEM it was necessary to carefully isolate microsamples corresponding to previously SEM-BSE-EDS-examined microzones followed by ultrathin sectioning of the samples. In order to do this, the undisturbed microsamples were excised from these thin sections under light microscopy and re-embedded in Araldite resin under vacuum (Wierzchos and Ascaso 1998). After polymerization, sections 50–70 nm thick were obtained using an ultramicrotome (diamond knife). These ultrathin sections were then placed on gold TEM grids, stained with lead citrate, and intercalated with *n*-alkylammonium chlorides ($n = 7$ and 18 carbon atoms in the alkyl chains, respectively). This treatment allows the determination of diagenetic interstratified clay minerals. A detailed description of the intercalation procedure may be found in Wierzchos and Ascaso (1998). All samples were examined using a Zeiss EM 910 TEM operated in high resolution mode and at 120 kV. EDS qualitative microanalysis was simultaneously performed using a Link ISIS system.

Results

The SEM-BSE images of a transverse rock section showed the presence of a saxicolous lichen *Lecidea cancriformis* (Dodge et Barker) frequently accompanied by bacterial cells. Microdivided minerals, such as biotite layers, and quartz and plagioclase grains derived from underlying rock could be seen within the lichen thallus. Fungal hyphae and chasmoendolithic colonies of bacteria were often observed inside fissures and cracks. In the deeper fissures of up to 5 mm, it was possible to observe extracellular coatings in the form of small spheres around the cross-sectioned hyphal cells (white arrows in Figure 1a). Using EDS point microanalysis, these inorganic deposits were found to contain high amounts of

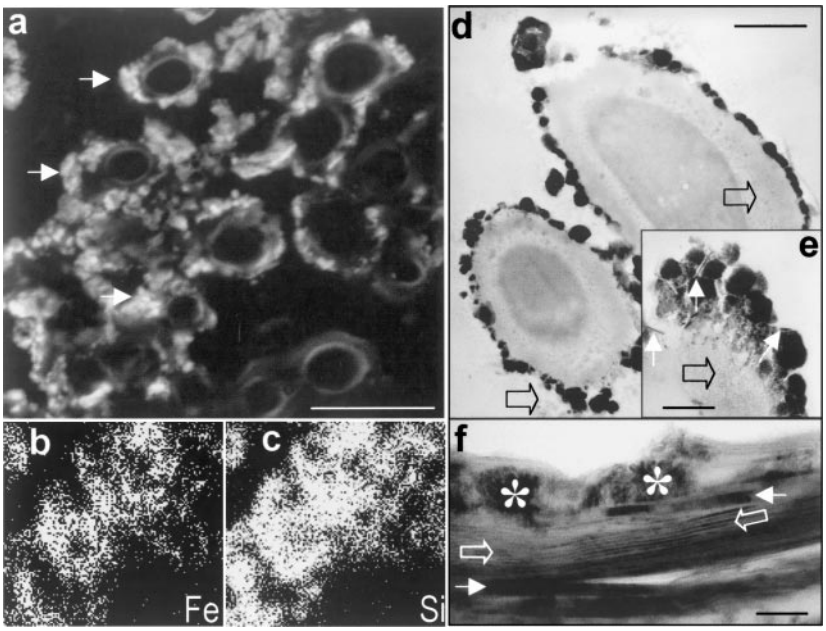

FIGURE 1 Diagenetic Fe-oxyhydroxide and aluminosilicate deposits around live hyphal cells (H). (a) SEM-BSE image of sphere-like extracellular coating materials (arrows). Scale bar = 5 μm. (b and c) EDS spatial distribution of Fe and Si, respectively, corresponding to Figure 1a. (d and e) TEM images of hyphal cells coated with subblocky grains of Fe-oxyhydroxides and thin layers of aluminosilicates (white arrows in Figure 1e); open arrows show Pb-composed nanoaggregates indicating the presence of polysaccharides. Scale bars = 1 and 0.5 μm, respectively. (f) HRTEM image of *n*-alkylammonium-treated, diagenetic, interstratified, vermiculitised, biotite-like clay around the hyphal cells and nanocrystalline Fe-oxyhydroxides (asterisks); white arrows—nonexpanded biotite with basal spaces of 10 Å and open arrows—expanded layers with basal spaces ranging from 16 to 20 Å identifying the deposit as vermiculite-like clay. Scale bar = 50 nm.

Fe and O along with lower levels of Si and Al, and traces of Na, Mg, K, and Ti. The Fe/Si distribution maps (Figures 1b–c) show that these major elements were evenly distributed around the hyphal cells. The morphological and crystallographic structure of these deposits around the live fungal sheaths was established by HRTEM (EDS) examination of extracted, re-embedded and ultrathin-sectioned hyphae from a rock fissure (Figures 1d–f). These images revealed two different phases within the secondary mineral coatings. First, there was a predominance of Fe-oxyhydroxide nanocrystals on the external surface of fungal hyphae in the form of small irregular subrounded grains, from 30–500 nm in size. Second, clays composed of Fe-rich aluminosilicate (white arrows in Figure 1e) could be seen in some of the spaces between these Fe-oxyhydroxide grains. The clays were identified by measurement of their lattice spacing. Untreated ultrathin sections showed the presence of clay particles with basal spaces measuring 10 Å. Following *n*-alkylammonium ion treatment (Wierzchos and Ascaso 1998) of the same material, many of the clay packets expanded forming interstratifications between the mineral layers (open arrows in Figure 1f). The presence of basal spaces 16 to 20 Å (most were around 17 Å) among these mineral layers of 10 Å basal space after *n*-alkylammonium ion treatment is a typical feature of interstratified vermiculitized biotite-like clays (Vali et al. 1992; Vali et al. 1994; Wierzchos and Ascaso 1998). No clay was observed within the fungal sheaths. The observation in some samples of Pb

aggregates (Pb is remobilized in the electron beam) demonstrated the presence of organic polymers, probably polysaccharide in nature (Barker and Banfield 1998), surrounding the Fe-oxyhydroxides and clays (open arrows in Figures 1d–e). Selected area electron diffraction analysis was performed on fine particle deposits found around the live fungal sheaths. However, it was only possible to observe a few reflections or very diffuse rings preventing positive mineral identification.

In situ SEM-BSE examination of another rock zone showed that some fissures were filled with abundant diagenetic deposits composed of Fe-rich aluminosilicate clays and thin bands of Fe-rich oxides (black arrows in Figure 2a and Fe distribution map in Figure 2b). These deposits occupied almost the entire width of the fissure. Several bacterial cells (black open arrow in Figure 2a) and hyphal cells (white open arrow in Figure 2a) with distinct ultrastructural elements were observed alongside these deposits. Several hyphal cells could also be seen within the clay—Fe-oxide matrix (white arrows in Figure 2a). However, the low sensitivity of these cells to Os and U cation staining indicated that they were biochemically inactive and consequently dead or decaying. Diagenetic clays and narrow bands of Fe-oxides occurred in discontinuous layers typically less then 0.3 μm thick, which usually developed in a c* direction, approximately in line with the long axis of the fissure. These diagenetic minerals formed outlines around the cells in close proximity to the decaying fungal sheaths. By EDS analysis, it was possible to detect Os and U within the diagenetic minerals indicating that microbial exopolymers are mixed with clay and Fe-oxides, since Os and U preferentially bind to the carboxyl groups of organic polymers (Foster 1981; Degens and Ittekkot 1982).

Another fissure contained Fe-rich aluminosilicate diagenetic deposits (Figure 2c), but no remains of microorganisms. These deposits presented a characteristic network-like structure, with preserved, elongated voids corresponding in size and shape to hyphal cells. The

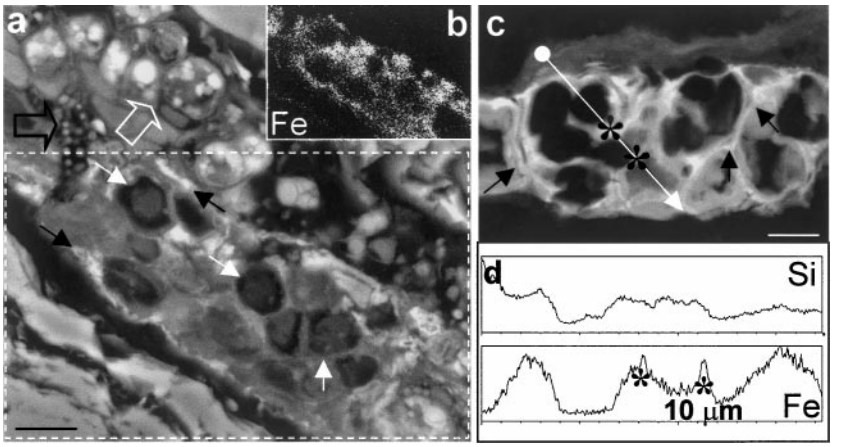

FIGURE 2 Diagenetic aluminosilicate clay and Fe-oxyhydroxide deposits around decaying hyphal cells. (a) SEM-BSE image of Fe-rich (black arrows) and aluminosilicate clay biomarkers within a deep granite rock fissure; white arrows—dead hyphal cells; black open arrow—live bacterial colony; white open arrow—live hyphal cells. Scale bar = 5 μm. (b) Spatial distribution of Fe corresponding to the boxed area in Figure 2a. (c) SEM-BSE image of network-like, Fe-rich aluminosilicate biomarkers with preserved membrane and wall structures (black arrows) of hyphal cells. Scale bar = 5 μm. (d) EDS microprobe scan-line corresponding to the arrow in Figure 2c shows a uniform relative Si concentration throughout the deposits and a higher relative Fe concentration (asterisks) in the area of the mineralized membrane and cell wall structures.

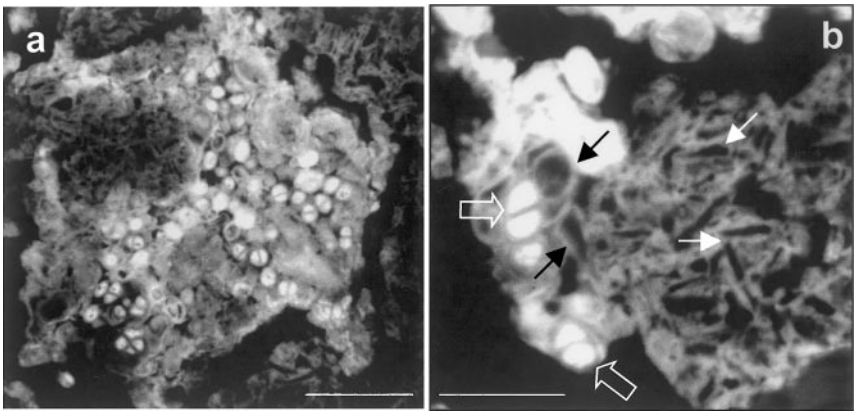

FIGURE 3 SEM-BSE images of endolithic bacteria and associated diagenetic Fe-rich deposits. (a) General view of bacterial colonies showing inorganic biomarkers. Scale bar = 5 μm. (b) Detailed view of the transitional process leading to the formation of Fe-rich diagenetic deposits: white open arrows—live bacteria, black arrows—Fe-rich bacterial ghosts, white arrows—inorganic collapsed bacterial biomarkers. Scale bar = 2 μm.

voids were surrounded mostly by Fe-oxides and Si-rich deposits (scan-lines in Figure 2d). Further detailed morphological examination of the inorganic deposits occupying the areas between voids revealed that most deposits were Fe-rich (asterisks in Figure 2c–d) and preserved the shape of membrane and cell wall structures (arrows in Figure 2c).

A colony of cocoidal chasmoendolithic bacteria was also observed in the rock fissure (Figures 3a–b). Bacteria were seen close to and/or within the extensive Fe-rich aluminosilicate deposits. A more detailed view of the bacterial cells (open arrows in Figure 3b) together with EDS examination showed that almost all these microorganisms were surrounded by Fe-oxides and, to a lesser extent, by aluminosilicate minerals with traces of Na, Mg, and K. In these cases, diagenetic minerals formed uniform, 0.2 μm-thick coatings around the bacterial cells (usually around clumps of 3 or 4 cells). After the death of the bacterium, these Fe-rich shells, or ghosts, appeared empty and eventually collapsed (arrows in Figure 3b) to form small, elongated inorganic structures. Accumulation of these structures produced characteristic sponge-like, Fe-rich aluminosilicate diagenetic deposits. These stages of bacterial decay and sponge-like structure formation may be observed in Figure 3b.

EDS analysis of the extracellular mineral deposits surrounding the live hyphae and bacterial cells and of the deposits considered to be biomarkers, showed Fe, Al, and Si to be the dominant components. Semiquantitative point EDS analysis established that the levels of Fe, Al, and Si were different in the mineral deposits associated with live and dead cells (Figure 4), with Fe content increasing, and Si and Al contents diminishing, as the bacterial cells died and decayed. These observations resemble those of previous studies on the composition of earlier stages of Fe-rich silicates surrounding bacterial cells from a freshwater environment (Tazaki 1997). Other studies performed on (Fe, Al)-silicate authigenetic minerals also suggest that Fe content increases in older crystalline, epicellular bacterial deposits in lake sediments (Ferris et al. 1987). However, Konhauser and Urrutia (1999) found that preferential accumulation of silica during the final stages of mineralization may also occur in aqueous biofilms. Quantitative changes were observed in the mineral composition of extracellular hyphal deposits (Figure 1a) and in the network-like Fe-rich aluminosilicate deposits (Figure 2c). Older deposits (no hyphal cells present) had reduced Fe and Al levels and increased Si levels (Figure 4).

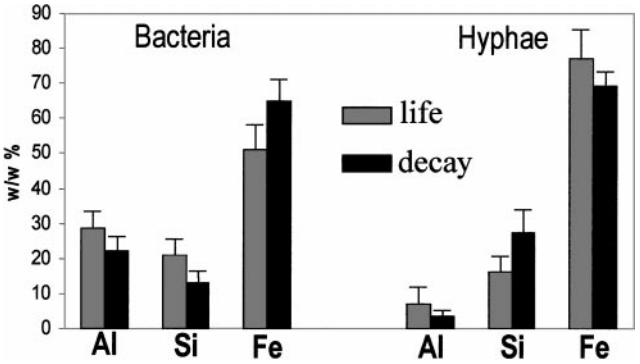

FIGURE 4 Comparison of the Al, Si, and Fe composition (wt %) of diagenetic, mineral deposits associated with live bacteria and hyphae (grey bars—EDS measurements performed on the areas showing live bacteria in Figure 3a and live hyphae in Figure 1a) and with decayed microorganisms (black bars—EDS measurements performed on inorganic deposits around bacteria shown in Figure 3a and around hyphae in Figure 2c).

The SEM-BSE image in Figure 5a shows one of the fossilized cells of an microorganism found within a deep Antarctic granite rock fissure associated with extensive biomineralization. The EDS scan-line showed that the cell wall mostly accumulated Fe (asterisks in Figures 5a–b) and that the cytoplasm was mainly filled with Si and Al (Figure 5b).

Discussion

The role of fungi and bacteria as nucleating agents for Fe-oxyhydroxide and in aluminosilicate formation can be attributed to their ability to immobilize cations and to give rise to fine-grained minerals (Nealson 1983; Fortin et al. 1997; Fortin and Ferris 1998; Fortin et al. 1998; Warren and Ferris 1998). The precipitation of minerals inside, outside, or even some distance away from bacterial cells has been related to both these processes (see review by Fortin et al. 1997). Bacteria can act as nucleation surfaces for Fe-rich minerals because their cell wall components have active amphoteric and amino groups. Alternatively, the

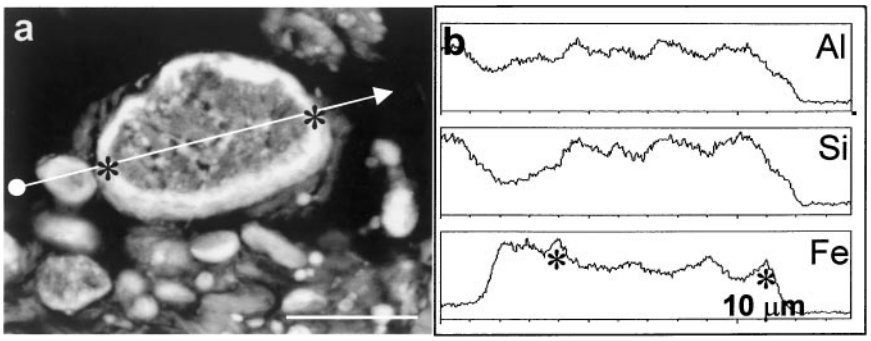

FIGURE 5 SEM-BSE image (a) of a fossilized Antarctic endolithic microorganism cell (scale bar $= 5\ \mu$m) and its Al, Si, and Fe composition shown by the EDS microprobe scan-line profile (b) along the white arrow drawn in Figure 5a; asterisks indicate the cell wall zone rich in Fe.

metabolic activity of some bacteria may change local redox and/or pH conditions leading to epicellular nucleation and mineral crystal growth on the outside of living or dead cells.

Initial stages of cationic element deposition in the vicinity of the microbial cell wall suggests binding to anionic surface polymers (Amouric and Parron 1985; Barker and Banfield 1996; Barker and Banfield 1998). Organic molecules such as polysaccharides are thought to have a significant role in low temperature mineral biotransformations, which leads to the dissolution, transport, and neocrystalization of minerals (Barker and Banfield 1996; Barker and Banfield 1998). Our results confirm that the process of mineral biotransformation via biochemical processes also occurs in the dry, low temperature environments of Antarctica. Polysaccharides are known to play a role as antidesiccants in microorganisms (Ophir and Gutnik 1994). Given the scarcity of water in this microhabitat, the activity of chasmoendolithic microorganisms involves strategies aimed at retaining the small amount of water available. This involves the production of high amounts of extracellular polysaccharides that, in turn, increases the rate of mineral biomobilization and biotransformation. When endoliths decay, the presence of Fe-rich diagenetic minerals could be interpreted as biomarkers, either because they contain remnants of ultrastructural cell elements or because it is possible to demonstrate the transition from deposits around live cells to deposits with no apparent cellular remains. This was shown here in the network-like inorganic deposits (Figure 2c), which are distinct biomarkers of the previous biological activity of chasmoendolithic fungal sheaths. This abundant accumulation of inorganic deposits are the result of Fe, Si, and Al biomobilization and biotransformation into diagenetic Fe-oxides and Si-rich minerals. Further, the well-preserved morphology of the membrane and cell wall structures within these deposits confirmed they were not abiogenic, but indeed biomarkers of previous hyphal cells activity.

Another clear example of biomarkers of chasmoendolithic Antarctic bacteria are the sponge-like neoformed Fe-rich mineral deposits observed behind the decayed bacterial cells (Figures 3a–b). Indeed, transition from deposits around live cell to deposits nonassociated with cells was unequivocally demonstrated on one occasion (Figure 3b). The observation that Fe-rich silicate sheets surrounded the live microcolony of bacteria suggests that the cell wall served as a nucleation surface. Silicate formation on bacterial surfaces has been reported in various aqueous environments (see review by Fortin et al. 1997). The present results indicate that some endolithic bacteria, when in a cold and dry environment, could also nucleate a variety of Fe-rich minerals. In a few cases, biomineralization of the cell of an endolithic microorganism was not restricted to its outer surface. Here, the entire cells becomes fossilized, exposing the outer surface Fe-rich sheath and Al, Si, and Fe-rich intracellular space (Figures 5a–b). Over their life span, these cells acquire an increasing mineral burden on their surfaces. When they die, this burden continues to increase until they become completely mineralized (Ferris et al. 1988). The authenticity of the features described as microfossils was established by their fulfilment of the criteria for "biogenicity" described by McKinley et al. (2000).

The structures observed were common and morphologically similar in size and shape to live photosynthetic microorganisms present in other fragments of this rock. Moreover, plausible ultrastructural elements such as thylakoid remains could be discerned in the SEM-BSE images. This may also confirm the dissimilarity of these structures with abiologic bodies. Given the presence of live endoliths within the rock, we consider that further criteria for microfossils such as association with biofilms and geologic and evolutionary contexts were also met. We conclude that these structures (Figure 5a) are indeed microfossils. These microfossils may remain as mineralized forms unless the geological horizon in which they are found is subjected to metamorphism over geological time. Thus, the processes

responsible for their formation as well as significant accumulation of Si in the cytoplasm have yet to be established.

The in situ examination of the inside of Antarctic rocks possibly represents the best option available to improve present knowledge of these traces of past life and to develop techniques for their recognition. Similar biomarkers might be expected to be present in Martian rocks even if all remnants of cells have vanished. This article represents a first step toward understanding the signs that Martian microbiota may have left for us to see.

References

Amouric M, Parron C. 1985. Structure and growth mechanisms of glauconite as seen by high resolution transmission electron microscopy. Clays Clay Miner 33:474–482.

Ascaso C, Wierzchos J. 1994. Structural aspects of the lichen-rock interface using backscattered electron imaging. Bot Acta 107:251–256.

Ascaso C, Wierzchos J, de los Rios A. 1995. Cytological investigations of lithobiontic microorganisms in granitic rocks. Bot Acta 108:474–481.

Barker WW, Banfield JF. 1996. Biologically versus inorganically-mediated weathering reactions: relationships between minerals and extracellular microbial polymers in lithobiontic communities. Chem Geol 132:55–69.

Barker WW, Banfield JF. 1998. Zones of chemical and physical interaction at interfaces between microbial communities and minerals: a model. Geomicrobiology 15:223–244.

Degens ET, Ittekkot VI. 1982. In situ metal staining of biological membranes in sediments. Nature 298:262–264.

Ferris FG, Fyfe WS, Beveridge TJ. 1987. Bacteria as nucleation sities for authigenetic minerals in a metal-contamined lake sediment. Chem Geol 63:225–232.

Ferris FG, Fyfe WS, Beveridge TJ. 1988. Metalic ion activity by Bacillus subtilis: implications for the fossilization of microorganisms. Geology 16:149–152.

Fortin D, Ferris FG, Beveridge TJ. 1997. Surface-mediated mineral development by bacteria. Rev Mineral 35:161–180.

Fortin D, Ferris FG. 1998. Precipitation of dissolved silica, sulfate and iron on bacterial surfaces. Geomicrob J 15:309–324.

Fortin D, Ferris FG, Scott SD. 1998. Formation of Fe-silicates and Fe-oxides on bacterial surfaces in samples collected near hydrothermal vents on the Southern Explorer Ridge in the northeast Pacific Ocean. Am Miner 83:1399–1408.

Foster RC. 1981. Polysaccharides in soil fabric. Science 214:665–667.

Friedmann EI. 1982. Endolithic microorganisms in the Antarctic cold desert. Science 215:1045–1053.

Friedmann EI, Weed R. 1987. Microbial trace-fossil formation, biogenous, and abiotic weathering in the Antarctic cold desert. Science 236:645–752.

Friedmann EI, Hua M, Ocampo-Friedmann R. 1988. Cryptoendolithic lichen and cyanobacterial communities of the Ross Desert, Antarctica. Polarforschung 58:251–259.

Joy DC. 1991. An introduction to Monte Carlo simulation. Scanning Microsc 5:329–337.

Kappen L. 1993. Lichens in the Antarctic region. In: Friedmann EI, editor. Antarctic Microbiology. New York: Wiley-Liss Inc. p 433–490.

Konhauser KO, Urrutia MM. 1999. Bacterial clay authigenesis: implications for river chemistry. Chem Geol 161:399–414.

McKay CP, Friedmann EI, Wharton RA, Davis WL. 1992. History of water on Mars: a biological perspective. Adv Space Res 12:231–238.

McKinley JP, Stevens TO, Westall F. 2000. Microfossils and paleoenvironments in deep subsurface basalt samples. Geomicrobiol J 17:43–54.

Nealson KH. 1983. The microbial iron cycle. In: Krumbein WE, editor. Microbial Geochemistry. Oxford London Edinburgh Boston Melbourne: Blackwell Scientific Publications. p 159–170.

Ophir T, Gutnik DL. 1994. A role for polysaccharides in the protection of microorganisms from dissection. Appl Environ Microbiol 60:740–745.

Øvstedal DO, Lewis Smith RI. 2001. Lichens of Antarctica and South Georgia. A guide to their identification and ecology, Cambridge, England: Cambridge University Press. 410 p.

Sun HJ, Friedmann EI. 1999. Growth on geological time scales in the Antarctic cryptoendolithic microbial community. Geomicrobiol J 16:193–202.

Tazaki K. 1997. Biomineralization of layer silicates and hydrated Fe/Mn oxides in microbial mats: an electron microscopical study. Clays Clay Miner 45:203–212.

Vali H, Hesse R, Kodama H. 1992. Arrangement of n-alkylammonium ions in phlogopite and vermiculite: an XRD and TEM study. Clays Clay Miner 40:240–245.

Vali H, Hesse R, Martin RF. 1994. A TEM-based definition of 2:1 layer silicates and their interstratified constituents. Am Miner 79:644–653.

Warren LA, Ferris FG. 1998. Continuum between sorption and precipitation of Fe(III) on bacterial cell surfaces. Environ Sci Technol 32:2331–2337.

Wierzchos J, Ascaso C. 1994. Application of back-scattered electron imaging to the study of the lichen-rock interface. J Microsc 175:54–59.

Wierzchos J, Ascaso C. 1996. Morphological and chemical features of bioweathered granitic biotite induced by lichen activity. Clays Clay Miner 44:652–657.

Wierzchos J, Ascaso C. 1998. Mineralogical transformation of bioweathered granitic biotite, studied by HRTEM: evidence for a new pathway in lichen activity. Clays Clay Miner 46:446–452.